Available online at www.sciencedirect.com
SCIENCE DIRECT®
Graphical Models 67 (2005) 260–284
Graphical Models
www.elsevier.com/locate/gmod

# A new characterization of simple elements in a tetrahedral mesh

Isabelle Bloch[a,*], Jérémie Pescatore[a,b,1], Line Garnero[b]

[a] *Ecole Nationale Supérieure des Télécommunications, Département TSI - CNRS UMR 5141 LTCI, IFR 49, 46 rue Barrault, 75013 Paris, France*
[b] *LENA, CNRS UPR 640, IFR 49, Hôpital La Salpétrière, 75 651 Paris Cedex 13, France*

Received 5 September 2003; received in revised form 12 August 2004; accepted 16 December 2004
Available online 12 February 2005

**Abstract**

This paper deals with topological analysis of sets of tetrahedra (''tetrahedral meshes'' of three-dimensional objects). We introduce a definition of simple elements for any normal tetrahedral representation. Then we prove a local characterization of simple tetrahedra in the case of a scene composed of one object and its background, based on homology groups and on relative homology. This allows us to define homotopic deformations of a tetrahedral representation. Using this characterization, we illustrate the problem of generating three-dimensional finite element meshes from medical voxel datasets.


*Keywords:* 3D topology; Tetrahedral mesh; Finite element meshes; Simple tetrahedron; Local topological characterization; Homology

* Corresponding author. Fax: +33 1 45 81 37 94.
*E-mail addresses:* Isabelle.Bloch@enst.fr (I. Bloch), Jeremie.Pescatore@med.ge.com (J. Pescatore), Line.Garnero@chups.jussieu.fr (L. Garnero).
[1] Present address: General Electric Medical Systems, Buc, France.

1524-0703/$ - see front matter 
doi:10.1016/j.gmod.2004.12.001

## 1. Introduction

This paper deals with three-dimensional (3D) digital topology. More specifically, it deals with topological properties of sets of tetrahedra, i.e., "tetrahedral meshes" of 3D objects. Digital topology provides a sound mathematical basis for various image processing applications including object classification, counting and labeling, border tracking, contour filling, thinning, and segmentation. An important property of topological parameters is that they are invariant under translation, rotation, shrinking, and more generally under elastic deformations. This property underlies the importance of topological parameters in analyzing images of biological organs. The analysis of 3D digital images has generated increasing interest with the rapid growth of 3D image processing and computer vision applications in several domains, including medical imaging. In medical imaging, techniques like computed tomography (CT), magnetic resonance imaging (MRI), positron emission tomography (PET), etc. are widely used to produce 3D digital images that carry much important information about anatomy and function of the human body. Udupa [1], among others, has discussed the applications of digital topology in 3D medical imaging.

A 3D digital image, in general, is a discrete subdivision of the 3D Euclidean space into elementary regions. Several types of representations are commonly used for 3D digital images: voxel representations and tetrahedral representations, which are both volumetric representations, surface representations, or cellular complexes that represent elements of different local dimensions. Most of the work on digital topology and 3D image processing makes use of voxel representations. Much less use has been made of the other representations, especially tetrahedral representations. Over a decade ago, Boissonnat [2] presented a method producing tetrahedral representations of 3D objects from their planar cross sections. But 3D volumes can also be used directly to produce meshes.

In this paper, we will study tetrahedral representations, which are defined by finite sets of tetrahedra (not necessarily regular).

One of the motivations to work on tetrahedral meshes concerns applications based on EEG and MEG data, where electromagnetic field propagation has to be calculated numerically, for instance using finite element methods. This computation is based on a meshed model of the head tissues. Examples of such models are shown in Fig. 1. Although spherical models lead to analytical expressions of electrical potentials and magnetic fields, they are not realistic and oversimplified. Realistic models can be built from anatomical (typically MRI) images of the subject under study. The meshed model can then be constructed from a segmentation of main tissues in such images, as illustrated in Fig. 2. Such applications require a labeling of the mesh where each tetrahedron receive a label corresponding to the majority tissue in the corresponding volume, while preserving the topological arrangement of the tissues (see the general scheme for the whole procedure in Fig. 3). The literature concentrates mainly on mesh construction, refinement, adaptation, but not on topological aspects.

One important notion is the characterization of simple elements, i.e., that can be added to or suppressed from an object without changing the topology. This allows us to perform the above mentioned labeling through a sequence of homotopic deforma-

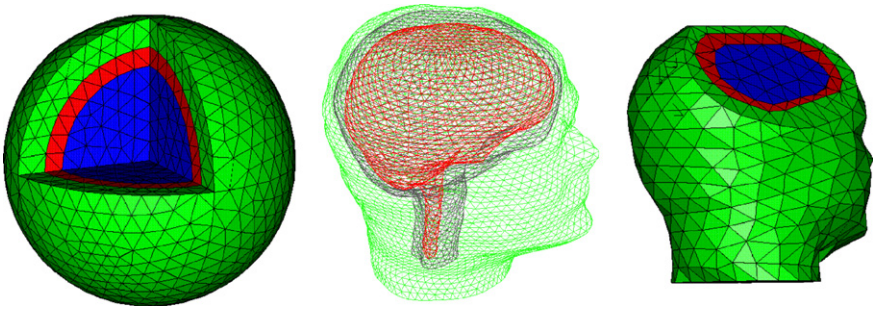

Fig. 1. A few examples of head models (from [3]): spherical model, homogeneous realistic surfacic model, and volumetric realistic model (enabling to consider anisotropy and heterogeneity).

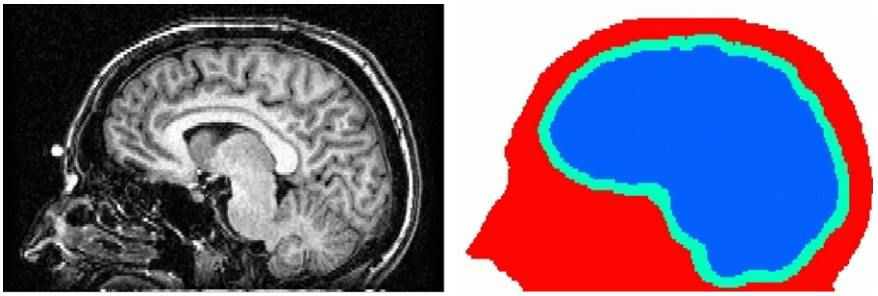

Fig. 2. MRI image (Pitié-Salpétrière Hospital) and segmentation of scalp, skull and brain (one slice of the 3D volume).

tions. Local characterizations exist for voxel representations and for cellular complexes, but not for tetrahedral representations [4–9].

This paper deals with the local topological analysis of tetrahedral representations. Following Kong [10], we define the simplicity of a tetrahedron $T$ as follows:

**Definition 1.** Let $T$ be a tetrahedron and $O$ a connected set of tetrahedra. The tetrahedron $T$ is said to be *simple* if the inclusion mapping $i: O \to O \cup T$ (i.e., the identity restricted to $O$) is a homotopy equivalence.

This definition is rarely used directly, because the condition in this definition is not easy to check in general. For voxel and cellular complex representations, the simplest local characterization consists in counting the connected components in the neighborhood of the considered point. To extend this notion to tetrahedral meshes, we rely on homology groups to find a local characterization of simple tetrahedra. The major result of this paper consists of this characterization. Although its expression is quite simple and intuitive since it only consists in checking simple conditions on the neighborhood of a tetrahedron (see Theorem 15), the proof is not straightforward: it can not rely on the usual notion of homotopy (as for voxels or cellular complexes), but we have to use more complex notions of homology and relative homology.

Basic concepts and definitions related to tetrahedral representations are presented in Section 2. In Section 3, we compute the homology groups of a tetrahedral mesh

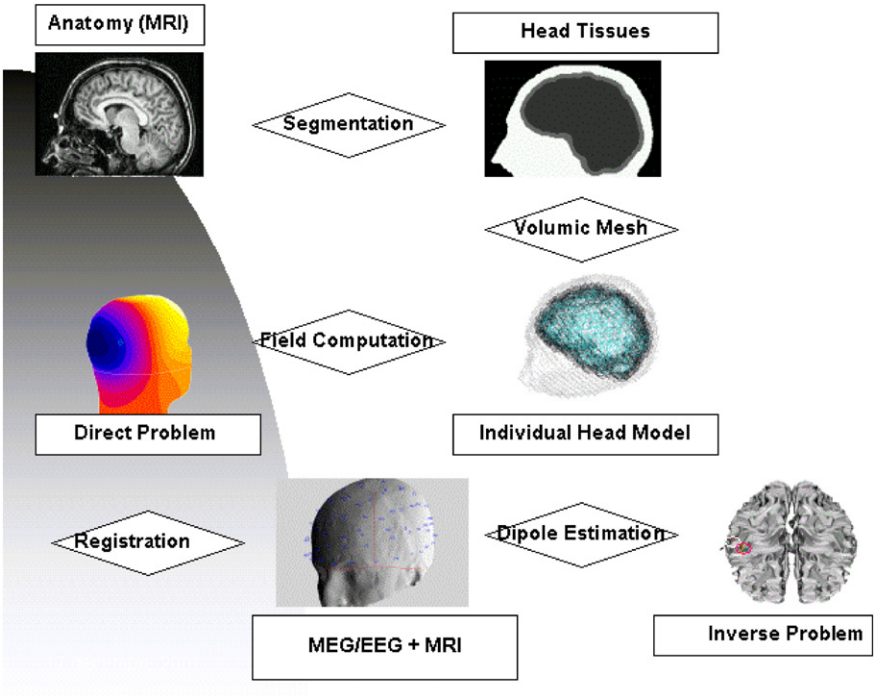


Fig. 3. General scheme in MEG/EEG direct and inverse problems: a head model is constructed from the patient's anatomy by segmenting a MRI image and building a labeled mesh.

(TM). Based on this result, a characterization of a simple element is developed in Section 4. Finally, Section 5 presents an application of our characterization of simple tetrahedra in medical imaging, aiming at constructing finite element (FE) meshes for electro-magnetic finite element models of the head tissues.

## 2. Basic concepts and definitions

We consider the 3D Euclidean space $\mathbb{R}^3$. A (closed) tetrahedron $T$ is defined by a quadruple $(v_1, v_2, v_3, v_4)$ of non-coplanar vertices (points of $\mathbb{R}^3$). An edge $e$ of the tetrahedron is defined by a pair $(v_i, v_j)$ of distinct vertices, and a face $f$ is defined by a triple $(v_i, v_j, v_k)$ of distinct vertices. It is worth mentioning that the terms "tetrahedron," "face," and "edge" do not denote the finite sets of vertices, but rather the closed convex hulls of those vertices. They are therefore 3D, 2D, and 1D entities, respectively, and contain their boundaries (e.g., an edge includes its two end points). Vertices, edges, faces, and tetrahedra are also referred to as 0-, 1-, 2-, and 3-simplexes, respectively. We define $interior(T)$ as $T$ without its faces. If $f$ is a face of $T$, we define $interior(f)$ as $f$ without its edges, and if $e$ is an edge of $T$, we define $interior(e)$ as $e$ without its vertices. Note that the interior of a 0-simplex (vertex) is empty.

A finite set $O$ of tetrahedra is called a *tetrahedral mesh* (TM) if the intersection of any two of its tetrahedra is either empty or it is a face, an edge or a vertex of both tetrahedra. It may be noted that a finite set $O$ of tetrahedra is a TM if and only if it constitutes a simplicial complex [11]. In the following, we will always consider TM. We express now the notion of connectivity in a TM.

A $k$-simplex ($k < 3$) $s$ of $O$ is *shared* if there exist two distinct tetrahedra $T_i$ and $T_j$ of $O$ such that $s \subseteq T_i \cap T_j$. Otherwise, $s$ is called *bare*. In particular, if a $k$-simplex $s$ is shared then the $k$-simplexes $s_i$ included in $s$ are also shared. For example, if a face is shared, then its edges are also shared. The two tetrahedra $T_i$ and $T_j$ sharing a $k$-simplex are said to be *neighbors*. Two tetrahedra are *adjacent* if they are distinct and share a vertex. Two tetrahedra are *edge-adjacent* if they are distinct and share an edge. Two tetrahedra are *face-adjacent* it they are distinct and share one face.

More generally, two simplexes $s_1$ and $s_2$ are said to be adjacent if and only if $s_1 \cap s_2 \neq \emptyset$.

A sequence $s_1, s_2, \ldots, s_n$ of simplexes in which $s_i$ is adjacent to $s_{i+1}$ for $1 \leqslant i < n$ is called a *path* from $s_1$ to $s_n$. The path is said to *join* the mesh elements $s_1$ and $s_n$.

A set $O$ of tetrahedra is *connected* if any two tetrahedra $T$ and $T'$ of $O$ are joined by a path of simplexes $T = s_0, s_1, \ldots, s_n = T'$ in $O$ such that $s_i$ and $s_{i+1}$ are adjacent for $0 \leqslant i < n$. If $O$ is a non-empty set of tetrahedra, then a *connected component* of $O$ is a maximal connected subset of $O$. Thus, every element of a non-empty set of tetrahedra lies in a unique component of $O$, and $O$ is connected if and only if $O$ has just one component.

Let $O$ be a TM and $T$ a tetrahedron of $O$, then:

- the neighborhood $N(T)$ of $T$ is defined as the union of all the tetrahedra $T_i \in O$ such that $T_i \cap T \neq \emptyset$,
- the *boundary* of $T$, denoted by $Bd\,T$, is the union of all the faces of $T$,
- the union of all the *shared* $k$-simplexes ($k < 3$) of $T$, denoted by $Bd_s\,T$, is called *the attachment* set of $T$,
- the union of the interiors of the *bare* $k$-simplexes ($k < 3$) of $T$, denoted by $Bd_b\,T$ is the *bare* boundary of $T$, and is actually the complement of the attachment set of $T$ in $Bd\,T$.

We illustrate the above definitions in Fig. 4. The tetrahedron $(a,b,c,d)$ has two bare faces $(a,b,c)$ and $(a,c,d)$ and two shared faces $(a,b,d)$ and $(b,c,d)$. This tetrahedron also has one shared edge $(a,c)$. Therefore, $Bd_b(a,b,c,d) = interior(a,b,c) \cup interior(a,c,d)$ and $Bd_s(a,b,c,d) = (a,b,d) \cup (b,c,d) \cup (a,c)$. Note that $Bd_b$ may also contain the interior of an edge; for example, in Fig. 4, $Bd_b(a,c,g,h) = interior(a,c,g) \cup interior(c,g,h) \cup interior(a,c,h) \cup interior(c,g) \cup interior(c,h)$.

## 3. Homology groups of a tetrahedral mesh

The characterization of simple elements is crucial for defining deformations of an object that preserve the topology. If the object is defined on a voxel grid, then local

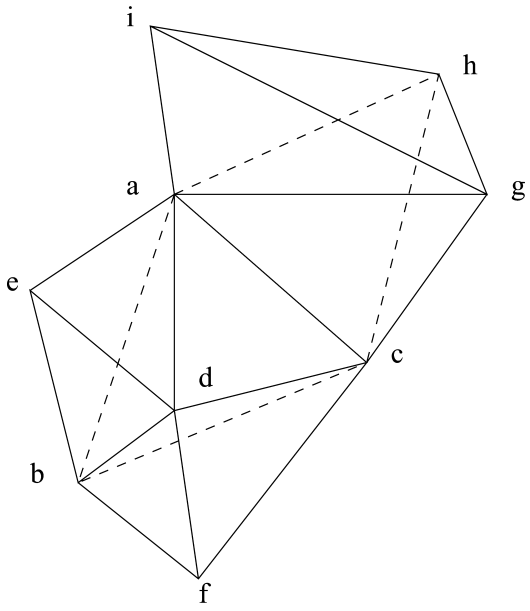


Fig. 4. Illustration of neighborhood of a tetrahedron.

characterizations exist based on the intersections between the neighborhood of a point and the object or its complement. They consist in checking that the neighborhood of a point has exactly one connected component in the object and one connected component in the background [5,4]. One problem is to define the appropriate connectivity to avoid topological paradoxes. Similar characterizations exist for cellular complexes [12,8]. Such structures deal in an elegant way with the topological paradoxes and do not require to define different connectivities for objects and background. Here again, the characterization of a simple element consists in checking that the neighborhood of the considered element has exactly one connected component in the object and one connected component in the background. This condition is necessary for any graph structure, and necessary and sufficient in case of cellular complexes due to the triangulated structure of the neighborhood [8]. For both voxels and cellular complexes, the notion of homotopy and related concepts is sufficient to derive these characterizations. Unfortunately, this is not the case for tetrahedral meshes, and the more complex notion of homology has to be used.

The mathematical structures underlying homology groups are *finitely generated groups*. Throughout this section, the group operation is denoted by $+$, all considered groups are Abelian (i.e., commutative), and the unit element is denoted by 0.

### 3.1. Chain group

We first define *orientations* of a $k$-simplex for $k \geqslant 1$. An oriented 1-simplex $s_1 = (p_0 p_1)$ is a directed line segment traversed in the direction $p_0 \to p_1$. Now

$(p_0p_1)$ can be distinguished from $(p_1p_0)$. We set $(p_0p_1) = -(p_1p_0)$. Here the symbol "$-$" in front of $(p_1p_0)$ should be understood in the sense of Abelian groups. The 1-simplex $(p_1p_0)$ is the *inverse* of $(p_0p_1)$: $(p_0p_1) + (p_1p_0) = 0$. Similarly, an oriented 2-simplex $s_2 = (p_0p_1p_2)$ is a triangle with oriented edges. The orientation of $(p_0p_1p_2)$ is the same as the one of $(p_2p_0p_1)$ or $(p_1p_2p_0)$, but opposite to the one of $(p_0p_2p_1)$, $(p_2p_1p_0)$ or $(p_1p_0p_2)$. Similarly, an oriented 3-simplex $(p_0p_1p_2p_3)$ is an ordered sequence of four vertices of a tetrahedron.

We now construct a group structure based on a oriented set of simplexes.

**Definition 2.** Let $O$ be a set of oriented $k$-simplexes with $k \leqslant 3$. Let $G_{I_r}$ be the set of oriented simplexes $s_{r,i}$ of dimension $r$ of $O$ in which a simplex appears with an unique orientation $(s_{r,i} \in G_{I_r} \Rightarrow -s_{r,i} \notin G_{I_r})$. We set $I_r = card(G_{I_r})$.

We construct a finitely generated group $C_r(O)$ which is generated by the elements of $G_{I_r}$, by defining at the same time the group law $+$ and an isomorphism $c_r : C_r(O) \to \mathbb{Z}^{I_r}$, by:

$$\begin{cases} c_r(s_{r,i}) = (0 \cdots 1_i \cdots\cdots 0), \\ c_r(-s_{r,i}) = -c_r(s_{r,i}), \\ c_r(s_{r,i} + s_{r,j}) = c_r(s_{r,i}) + c_r(s_{r,j}), \\ c_r(0) = (0 \cdots 0 \cdots\cdots 0), \end{cases}$$

where $1_i$ corresponds to the 1 a the $i$th position.

If $r > k$, we set $C_r(O) = \{0\}$.

The group $C_r(O)$ is called the *r-chain group* and every element of $C_r(O)$ is called an *r-chain*. Any element of $C_r(O)$ can be written formally as $\sum_{i=1}^{I_r} n_i s_{r,i},\ n_i \in \mathbb{Z}$, and is mapped by $c_r$ to $(n_1, \ldots, n_{I_r}) \in \mathbb{Z}^{I_r}$.

Let us now compute the chain groups of a tetrahedron and its boundary.

An oriented tetrahedron $T$ contains the following set of oriented $k$-simplexes:

$$T = \left\{ \begin{array}{c} p_0, p_1, p_2, p_3, \\ (p_0p_1), (p_0p_2), (p_0p_3), (p_1p_2), (p_1p_3), (p_2p_3), \\ (p_0p_1p_2), (p_0p_1p_3), (p_0p_2p_3), (p_1p_2p_3), \\ (p_0p_1p_2p_3) \end{array} \right\}.$$

The boundary $Bd\,T$ of the oriented tetrahedron $T$ is an example of a simplicial complex, built out of four 0-simplexes, six 1-simplexes, and four 2-simplexes. Thus,

$$Bd\,T = \left\{ \begin{array}{c} p_0, p_1, p_2, p_3, \\ (p_0p_1), (p_0p_2), (p_0p_3), (p_1p_2), (p_1p_3), (p_2p_3), \\ (p_0p_1p_2), (p_0p_1p_3), (p_0p_2p_3), (p_1p_2p_3) \end{array} \right\}.$$

As $T$ and $Bd\,T$ have the same oriented $r$-simplexes for $r < 3$, $C_r(T) = C_r(Bd\,T)$. Thus, the chain groups of $T$ and the surface $Bd\,T$ of a tetrahedron $T$ are:

$$C_0(T) = C_0(Bd\,T) = \{n_0p_0 + n_1p_1 + n_2p_2 + n_3p_3 / (n_0 \ldots n_3) \in \mathbb{Z}^4\}, \tag{1}$$

$$C_1(T) = C_1(Bd\,T) = \{n_0(p_0p_1) + n_1(p_0p_2) + n_2(p_0p_3) + n_3(p_1p_2) + n_4(p_1p_3) + n_5(p_2p_3)/(n_0 \ldots n_5) \in \mathbb{Z}^6\}, \quad (2)$$

$$C_2(T) = C_2(Bd\,T) = \{n_0(p_0p_1p_2) + n_1(p_0p_1p_3) + n_2(p_0p_2p_3) + n_3(p_1p_2p_3)/(n_0 \ldots n_3) \in \mathbb{Z}^4\}, \quad (3)$$

$$C_3(T) = \{n_0(p_0p_1p_2p_3)/n_0 \in \mathbb{Z}\}, \quad (4)$$

$$C_3(Bd\,T) = \{0\}, \quad (5)$$

$$C_r(T) = C_r(Bd\,T) = \{0\} \text{ for } r \geqslant 4. \quad (6)$$

### 3.2. Boundary operator

Let us now introduce the boundary operator $\partial_k$ and the boundary $\partial_k s_k$ of a $k$-simplex $s_k$.

Since a 0-simplex has no boundary, we define $\partial_0 p_0 = 0$. For a 1-simplex $(p_0p_1)$, we define $\partial_1(p_0p_1) = p_1 - p_0$.The minus sign in front of $p_0$ is related to the orientation. The following examples will clarify this point. In Fig. 5, an oriented 1-simplex $(p_0p_2)$ is divided into two simplexes, $(p_0p_1)$ and $(p_1p_2)$. The boundary of $(p_0p_2)$ should clearly consist of the vertices $p_0$ and $p_2$. This is achieved by the definition of $\partial_1$ and the minus sign, which eliminates the fictitious boundary $p_1$: $\partial_1(p_0p_1) + \partial_1(p_1p_2) = p_1 - p_0 + p_2 - p_1 = p_2 - p_0$ as expected. Another example is the triangle in Fig. 5. It is the sum of three oriented 1-simplexes, $(p_0p_1) + (p_1p_2) + (p_2p_0)$, and

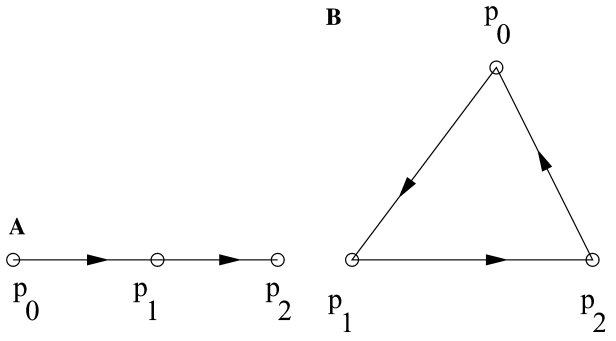


Fig. 5. (A) An oriented 1-simplex with a fictitious boundary $p_1$ and (B) a simplicial complex $O$ where the element $c = (p_0p_1) + (p_1p_2) + (p_2p_0) \in C_1(O)$ is a 1-cycle.

has intuitively no boundary because it is a cycle (a loop). Indeed we get: $\partial_1(p_0p_1) + \partial_1(p_1p_2) + \partial_1(p_2p_0) = p_1 - p_0 + p_2 - p_1 + p_0 - p_2 = 0$ as expected. This is generalized for any $r$-simplex as follows:

**Definition 3.** Let $s_r = (p_0 \dots p_r)(r > 0)$ be an oriented $r$-simplex. The *boundary* $\partial_r s_r$ of $s_r$ is a $(r-1)$-chain defined as:

$$\partial_r s_r = \sum_{i=0}^{r} (-1)^i (p_0 p_1 \dots \widehat{p_i} \dots p_r),$$

where the point $p_i$ under the symbol $\widehat{\ }$ is omitted. We also define $\partial_0 s_0 = 0$.

The operator $\partial_r$ acts linearly on an element $c = \sum_{i=1}^{I_r} c_i s_{r,i}$ of $C_r(O)$, i.e., $\partial_r c = \sum_{i=1}^{I_r} c_i \partial_r s_{r,i}$. The mapping $\partial_r : C_r(O) \to C_{r-1}(O)$ is called the *boundary operator* and is a homomorphism [11,13].

Based on this operator, two subgroups of $C_r(O)$ can be defined, respectively, the kernel of $\partial_r$ and the image of $\partial_{r+1}$.

### 3.3. Cycle group

**Definition 4.** If $c \in C_r(O)$ and $\partial_r c = 0$, $c$ is called a *r-cycle*. The set of $r$-cycles $Z_r(O) = ker\,\partial_r$ is a subgroup of $C_r(O)$ and is called the *r-cycle group*.

Let us compute the $r$-cycle groups of $T$ and $Bd\,T$. As $T$ and $Bd\,T$ have the same oriented $r$-simplexes for $r < 3$, $Z_r(T) = Z_r(Bd\,T)$. First,

$$Z_0(T) = Z_0(Bd\,T) = C_0(T) = C_0(Bd\,T). \tag{7}$$

since the boundary of any 0-simplex is 0.

The computation of $Z_1(T) = Z_1(Bd\,T)$ is a little bit more tedious. Any $z$ of $C_1(T)$ can be written in the following form [see Eq. (2)]:

$$z = n_0(p_0p_1) + n_1(p_0p_2) + n_2(p_0p_3) + n_3(p_1p_2) + n_4(p_1p_3) + n_5(p_2p_3).$$

Then we have:

$$\begin{aligned}
& z \in Z_1(T) \Longleftrightarrow \partial_1 z = 0 \\
& \Longleftrightarrow n_0(p_1 - p_0) + n_1(p_2 - p_0) + n_2(p_3 - p_0) + n_3(p_2 - p_1) \\
& \qquad + n_4(p_3 - p_1) + n_5(p_3 - p_2) = 0 \\
& \Longleftrightarrow \begin{cases} -n_0 - n_1 - n_2 = 0 \\ n_0 - n_3 - n_4 = 0 \\ n_1 + n_3 - n_5 = 0 \\ n_2 + n_4 + n_5 = 0 \end{cases} \\
& \Longleftrightarrow \begin{cases} n_5 = n_1 + n_3 \\ n_4 = n_0 - n_3 \\ n_2 = -n_0 - n_1. \end{cases}
\end{aligned}$$

Thus $z = n_0(p_0p_1 + p_1p_3 + p_3p_0) + n_1(p_0p_2 + p_2p_3 + p_3p_0) + n_3(p_1p_2 + p_2p_3 + p_3p_1)$, $p_3p_0) + n_1(p_0p_2 + p_2p_3 + p_3p_0) + n_3(p_1p_2 + p_2p_3 + p_3p_1)$, and $Z_1(T)$ is therefore generated by the following cycles: $p_0p_1 + p_1p_3 + p_3p_0$, $p_0p_2 + p_2p_3 + p_3p_0$, $p_1p_2 + p_2p_3 + p_3p_1$, and can be written as:

$$\begin{aligned} Z_1(T) &= Z_1(Bd\,T) \\ &= \{n_0(p_0p_1 + p_1p_3 + p_3p_0) + n_1(p_0p_2 + p_2p_3 + p_3p_0) \\ &\quad + n_3(p_1p_2 + p_2p_3 + p_3p_1)/(n_0, n_1, n_3) \in \mathbb{Z}^3\}. \end{aligned} \tag{8}$$

Intuitively, it corresponds to the subgroup of $C_1(T)$ generated by the cycles defined by the faces of $T$.

Let us now compute $Z_2(T) = Z_2(Bd\,T)$. Let $z = n_0(p_0p_1p_2) + n_1(p_0p_1p_3) + n_2(p_0p_2p_3) + n_3(p_1p_2p_3) \in C_2(T)$, with $(n_0 \dots n_3) \in \mathbb{Z}^4$ [Eq. (3)].

$$\begin{aligned} & z \in Z_2(T) \Longleftrightarrow \partial_2 z = 0 \\ & \Longleftrightarrow n_0((p_1p_2) - (p_0p_2) + (p_0p_1)) + n_1((p_1p_3) - (p_0p_3) + (p_0p_1)) \\ & \quad + n_2((p_2p_3) - (p_0p_3) + (p_0p_2)) + n_3((p_2p_3) - (p_1p_3) + (p_1p_2)) = 0 \\ & \Longleftrightarrow (n_0 + n_3)(p_1p_2) + (n_2 - n_0)(p_0p_2) + (n_0 + n_1)(p_0p_1) + (n_1 - n_3)(p_1p_3) \\ & \quad - (n_1 + n_2)(p_0p_3) + (n_2 + n_3)(p_2p_3) = 0. \end{aligned}$$

This equation is satisfied if and only if $n_0 = n_2$, $n_3 = n_1$, and $n_0 = -n_1$. Thus

$$\begin{aligned} Z_2(T) &= Z_2(Bd\,T) \\ &= \{n_0(p_0p_1p_2) - n_0(p_0p_1p_3) + n_0(p_0p_2p_3) - n_0(p_1p_2p_3)/n_0 \in \mathbb{Z}\}. \end{aligned} \tag{9}$$

It follows that $Z_2(T)$ and $Z_2(Bd\,T)$ are isomorphic to $\mathbb{Z}$.

Finally, for $r \geqslant 3$, we have $Z_r(T) = \{0\}$ and $Z_r(Bd\,T) = \{0\}$.

### 3.4. Boundary group

**Definition 5.** Let $c \in C_r(O)$. If there exists $d \in C_{r+1}(O)$ such that $c = \partial_{r+1}d$, then $c$ is called a $r$-boundary. The set of $r$-boundaries $B_r(O) = \operatorname{im}\partial_{r+1}$ is a subgroup of $C_r(O)$ and is called the *r-boundary group*.

It is easy to prove that $\partial_r\partial_{r+1} = 0$, and to deduce $B_r(O) \subseteq Z_r(O) \subseteq C_r(O)$.

Let us compute the $r$-boundary groups of $T$ and $Bd\,T$. Since $T$ and $Bd\,T$ have the same oriented $r$-simplexes for $r < 3$, we have $B_r(T) = B_r(Bd\,T)$ for $r < 2$. From Eq. (2) we have:

$$\begin{aligned} B_0(T) &= B_0(Bd\,T) \\ &= \{\partial_1[n_0(p_0p_1) + n_1(p_0p_2) + n_2(p_0p_3) + n_3(p_1p_2) + n_4(p_1p_3) + n_5(p_2p_3)]/ \\ &\quad (n_0 \dots n_5) \in \mathbb{Z}^6\} \\ &= \{n_0(p_1 - p_0) + n_1(p_2 - p_0) + n_2(p_3 - p_0) + n_3(p_2 - p_1) + n_4(p_3 - p_1) \\ &\quad + n_5(p_3 - p_2)/(n_0 \dots n_5) \in \mathbb{Z}^6\} \\ &= \{p_0(-n_0 - n_1 - n_2) + p_1(n_0 - n_3 - n_4) + p_2(n_1 + n_3 - n_5) \\ &\quad + p_3(n_2 + n_4 + n_5)/(n_0 \dots n_5) \in \mathbb{Z}^6\}. \end{aligned} \tag{10}$$

From Eq. (3) we have:

$$\begin{aligned}
B_1(T) &= B_1(BdT)\\
&= \{\partial_2[n_0(p_0p_1p_2)+n_1(p_0p_1p_3)+n_2(p_0p_2p_3)+n_3(p_1p_2p_3)]/(n_0\ldots n_3)\in\mathbb{Z}^4\}\\
&= \{n_0((p_1p_2)-(p_0p_2)+(p_0p_1))+n_1((p_1p_3)-(p_0p_3)+(p_0p_1))\\
&\quad +n_2((p_2p_3)-(p_0p_3)+(p_0p_2))+n_3((p_2p_3)-(p_1p_3)+(p_1p_2))/(n_0\ldots n_3)\in\mathbb{Z}^4\}\\
&= \{p_0p_1(n_0+n_1)+p_0p_2(-n_0+n_2)+p_0p_3(-n_1-n_2)+p_1p_2(n_0+n_3)\\
&\quad +p_1p_3(n_1-n_3)+p_2p_3(n_2+n_3)/(n_0\ldots n_3)\in\mathbb{Z}^4\}. \qquad (11)
\end{aligned}$$

$$\begin{aligned}
B_2(T) &= \{\partial_3\{n_0(p_0p_1p_2p_3)\}/n_0\in\mathbb{Z}\}\\
&= \{-n_0(p_0p_1p_2)+n_0(p_0p_1p_3)-n_0(p_0p_2p_3)+n_0(p_1p_2p_3)/n_0\in\mathbb{Z}\} \qquad (12)
\end{aligned}$$

and thus, $B_2(T)$ is isomorphic to $\mathbb{Z}$. Since there are no 3-simplexes in $BdT$, we have $B_2(BdT)=\{0\}$. Finally for $r\geqslant 3$, we have $B_r(T)=B_r(BdT)=\{0\}$.

### 3.5. Homology groups

The question now is to see how the three groups $C_r(O)$, $Z_r(O)$, and $B_r(O)$ associated with a TM are related to topological properties of the TM. Let us first consider a simple geometrical example: the edges of a triangle and those of a square are homeomorphic to each other but clearly $C_1(triangle)$ is isomorphic to $\mathbb{Z}^3$ and $C_1(square)$ is isomorphic to $\mathbb{Z}^4$. Hence $C_r(O)$ is not a topological invariant. Similar examples can be found to show that $Z_r(O)$ and $B_r(O)$ are not topological invariants either. But their quotient group provides the desired topological invariant, as shown below.

**Definition 6.** Let $O$ be a TM. The $r$th *homology group* $H_r(O)$, $0\leqslant r\leqslant n$, associated with $O$ is defined by:

$$H_r(O)=Z_r(O)/B_r(O),$$

where the quotient group is associated to the following equivalence relation: $z\sim z'$ if and only if $z-z'\in B_r(O)$. The quotient group is the set of equivalence classes of $r$-cycles, $H_r(O)=\{[z]|\, z\in Z_r(O)\}$ where each equivalence class $[z]$ is called a *homology class*. Two $r$-cycles $z$ and $z'$ such that $z\sim z'$ (or $[z]=[z']$) are said to be *homologous*.

Geometrically, $z-z'$ is a boundary of some space. The homology group $H_1(O)$ represents the set of closed curves in $O$ and the homology group $H_2(O)$ represents the set of closed surfaces in $O$. We can consider that homology groups allow us to count "cavities" in higher dimension spaces. For instance for the 2-unit sphere $S^2$, $H_1(S^2)=\{0\}$ since any closed curve of $S^2$ is the boundary of an element of dimension 2 in $S^2$, and $H_2(S^2)\neq\{0\}$ since no closed surface can be the boundary of an element of dimension 3.

We now recall some results concerning homology groups. They can be found in textbooks on topology and algebraic topology, such as [11] or [13] among many others.

**Theorem 7** ([11,13]). *Homology groups are topological invariants*: *let $X$ be homeomorphic to $Y$, then $H_r(X)$ is isomorphic to $H_r(Y)$.*

**Theorem 8** ([11,13]). *Let $O$ be a TM. Then $H_0(O)$ is isomorphic to $\mathbb{Z}^m$ where $m$ is the number of connected components of $O$.*

Let us now compute the $r$th homology group of a tetrahedron $T$ and its boundary $BdT$. Since $Z_r(T) = Z_r(BdT)$ and $B_r(T) = B_r(BdT)$ for $r \leqslant 1$, we have $H_0(BdT) = H_0(T)$ and $H_1(BdT) = H_1(T)$.

We have $Z_0(T) = C_0(T)$. From Eq. (10) we also have:

$$z = \sum_{j=0}^{3} a_j p_j \in B_0(T) \Longleftrightarrow \exists (n_0 \ldots n_5) \in \mathbb{Z}^6 / \begin{cases} a_0 = -n_0 - n_1 - n_2 \\ a_1 = n_0 - n_3 - n_4 \\ a_2 = n_1 + n_3 - n_5 \\ a_3 = n_2 + n_4 + n_5 \end{cases} \Longleftrightarrow \sum_{j=0}^{3} a_j = 0.$$

Let us define a surjective homomorphism $f : Z_0(T) \to \mathbb{Z}$ by:

$$f(a_0 p_0 + a_1 p_1 + a_2 p_2 + a_3 p_3) = \sum_{j=0}^{3} a_j.$$

We have $ker\ f = f^{-1}(0) = B_0(T)$. From the fundamental homomorphism theorem, $Z_0(T)/ker\ f$ is isomorphic to im $f$. Since im $f = \mathbb{Z}$, $H_0(T)$ is isomorphic to $\mathbb{Z}$ and $H_0(BdT)$ is isomorphic to $\mathbb{Z}$ too.

Let us show that $Z_1(T) = B_1(T)$. If $z \in B_1(T)$ then $z$ can be written in the following form [see Eq. (11)]:

$$\begin{aligned} z = {} & i((p_1p_2) - (p_0p_2) + (p_0p_1)) + j((p_1p_3) - (p_0p_3) + (p_0p_1)) + k((p_2p_3) \\ & - (p_0p_3) + (p_0p_2)) + l((p_2p_3) - (p_1p_3) + (p_1p_2)). \end{aligned} \tag{13}$$

On the other hand, if $z \in Z_1(T)$, then $z$ can be written in the following form [see Eq. (8)]:

$$z = n_0(p_0p_1 + p_1p_3 + p_3p_0) + n_1(p_0p_2 + p_2p_3 + p_3p_0) + n_3(p_1p_2 + p_2p_3 + p_3p_1). \tag{14}$$

From Eqs. (13) and (14), we have, for $z \in Z_1(T)$:

$$z \in B_1(T) \Longleftrightarrow \exists (i,j,k,l) \in \mathbb{Z}^4 / \begin{cases} (1)\, i + j = n_0, \\ (2)\, j - l = n_0 - n_3, \\ (3)\, j + k = n_0 + n_1, \\ (4)\, -i + k = n_1, \\ (5)\, k + l = n_1 + n_3, \\ (6)\, i + l = n_3. \end{cases}$$

Since $(5) = (4) + (6)$, $(3) = (2) + (5)$, $(2) = (3) - (5)$, the system is reduced to the three following independent equations:

$$z \in B_1(T) \Longleftrightarrow \exists (i,j,k,l) \in \mathbb{Z}^4 / \begin{cases} j = n_0 - i, \\ k = n_1 + i, \\ l = n_3 - i. \end{cases}$$

This system has an infinite number of solutions. Therefore, $Z_1(T) \subseteq B_1(T)$. Similarly, we can show that $B_1(T) \subseteq Z_1(T)$ and therefore $Z_1(T) = B_1(T)$. Thus $H_1(T) = Z_1(T)/Z_1(T)$ and so $H_1(T)$ is isomorphic to $\{0\}$, as well as $H_1(BdT)$.

From the previous section, we know that $Z_2(BdT)$ is isomorphic to $\mathbb{Z}$ and $B_2(BdT) = \{0\}$. Therefore, $H_2(BdT)$ is isomorphic to $\mathbb{Z}$. As for $H_2(T)$ computation, $Z_2(T)$ is isomorphic to $\mathbb{Z}$ and $B_2(T)$ is isomorphic to $\mathbb{Z}$. Therefore, $H_2(T)$ is isomorphic to $\{0\}$.

Table 1 summarizes the homology groups for a tetrahedron $T$ and its boundary $BdT$ ($\cong$ means isomorphic to).

Simple tetrahedra, developed in Section 4, are defined in this paper using the concept of a homotopy equivalence. Therefore, the following theorem gives the fundamental link between an homotopy equivalence and the homology group.

**Theorem 9** ([10]). *Let $O_1$ be a TM included in another TM $O_2$ ($O_1 \subseteq O_2$). If the inclusion mapping $i: O_1 \to O_2$ is a homotopic equivalence, then it induces isomorphisms $i_{r*}$ from the homology groups $H_r(O_1)$ to $H_r(O_2)$ for all $r = 0, 1, 2, \ldots$*

### 3.6. Relative homology

Similarly to the chain, cycle and boundary groups, it is possible to define relative chain, cycle and boundary groups when a TM is included in another TM.

**Definition 10** ([14]). Let $O_1$ be a TM included in another TM $O_2$ ($O_1 \subseteq O_2$). The *relative chain group* $C_r(O_2/O_1)$ is defined as the following quotient group:

$$C_r(O_2/O_1) = C_r(O_2)/C_r(O_1),$$

where a class of equivalence $\overline{c_r}$ is the set of all the $r$-chains $c_r + k_r$ (with $k_r$ a $r$-chain of $O_1$) of $O_2$.

A generic element of $C_r(O_2/O_1)$ will be denoted by $c + C_r(O_1)$.

Table 1
Homology groups $H_r(T)$ and $H_r(BdT)$

| TM | Homology group |
|---|---|
| $BdT$ | $H_0(BdT) \cong \mathbb{Z}$ |
| | $H_1(BdT) \cong \{0\}$ |
| | $H_2(BdT) \cong \mathbb{Z}$ |
| | $H_r(BdT) \cong \{0\}$ $r > 2$ |
| $T$ | $H_0(T) \cong \mathbb{Z}$ |
| | $H_1(T) \cong \{0\}$ |
| | $H_2(T) \cong \{0\}$ |
| | $H_r(T) = \{0\}$ $r > 2$ |

Then, we can define the following homomorphisms $\overline{\partial_r} : C_r(O_2/O_1) \to C_{r-1}(O_2/O_1)$ from the homomorphismn $\partial_r : C_r(O_2) \to C_{r-1}(O_2)$.

**Definition 11** ([11]). Let $O_1$ be a TM included in another TM $O_2 (O_1 \subseteq O_2)$. The mapping $\overline{\partial_r} : C_r(O_2/O_1) \to C_{r-1}(O_2/O_1)$ is the homomorphism defined by:

$$\overline{\partial_r}(c + C_r(O_1)) = \partial_r(c) + C_{r-1}(O_1) \quad \forall c \in C_r(O_2).$$

It can be shown that $\overline{\partial_r \partial_{r+1}} = 0$ and that im $\overline{\partial_{r+1}} \subseteq ker\overline{\partial_r}$. From the homomorphism $\overline{\partial_r}$, it is then possible to construct a relative group structure.

**Definition 12** ([11]). Let $O_1$ be a TM included in a TM $O_2$. The *relative homology groups* $H_r(O_2/O_1)$ are defined by:

$$H_r(O_2/O_1) = Z_r(O_2/O_1)/B_r(O_2/O_1) = \{[\overline{z}] \mid \overline{z} \in Z_r(O_2/O_1)\},$$

where:

- $Z_r(O_2/O_1) = ker\,\overline{\partial_r}$ are the relative cycle groups (where a chain $\overline{z}$ is a relative cycle if and only if $\overline{\partial_r z} = 0$),
- $B_r(O_2/O_1) = \text{im}\,\overline{\partial_{r+1}}$ are the relative boundary groups.

The relative homology groups allow for the construction of an exact sequence. A sequence of groups $G_i$ and homomorphisms $\psi_i : G_i \to G_{i-1}$ with $i = 2,\ldots$ is called an *exact sequence* if $\text{im}\,\psi_i = ker\psi_{i-1}$.

**Theorem 13.** ([11]) *Let $O_1$ be a TM included in a TM $O_2$. Let us consider*:

- *the homomorphisms $i_{r*} : H_r(O_1) \to H_r(O_2)$ induced by the inclusion mapping $i(v) = v$ for all $v \in O_1$,*
- *the homomorphisms $j_{r*} : H_r(O_2) \to H_r(O_2/O_1)$ induced by the canonical homomorphisms $j_r : C_r(O_2) \to C_r(O_2/O_1)$ (defined by $\forall c \in C_r(O_2), j_r(c) = c + C_r(O_1)$[2]), i.e., such that $j_{r*}([z_r]) = [j_r(z_r)]$,*
- *the homomorphisms $\partial_{r*} : H_r(O_2/O_1) \to H_{r-1}(O_1)$, defined by $\partial_{r*}(h) = \partial_r(c) + B_{r-1}(O_1)$, for $h = z + B_r(O_2/O_1)$ and $z = c + C_r(O_1)$ such that $c \in C_r(O_2)$, $\partial_r(c) \in C_{r-1}(O_1)$ or $\partial_r(c) = 0$.*

*The following sequence of groups and homomorphisms (called an homology sequence)* $\cdots \to_{i_{r*}} H_r(O_2) \to_{j_{r*}} H_r(O_2/O_1) \to_{\partial_{r*}} H_{r-1}(O_1) \to_{i_{r-1*}} H_{r-1}(O_2) \to_{j_{r-1*}} \cdots \to_{i_{0*}} H_0(O_2)$ *is exact.*

The following theorem is also an important topological result and will be used in Section 4.

**Theorem 14** ([11]). *Let $O_K$ be a TM, let $O_L$ be a TM included in $O_K$, let $O_{K_1}$ be a TM included in $O_K$ such that $O_{K_1}$ contains $(O_K - O_L)$ and let $O_{L_1}$ be a TM corresponding to*

[2] Note that we have $\forall r, j_{r-1}\partial_r = \overline{\partial_r} j_r$.

*the union of the shared simplexes of $O_{K_1}$ with $O_L$. The relative homology groups $H_r(O_{K_1}/O_{L_1})$ are isomorphic to the relative homology groups $H_r(O_K/O_L)$ for all r.*

From these results, we are now able to prove a characterization of a simple tetrahedron.

## 4. Characterization of a simple tetrahedron

As stated in the Section 1, Definition 1 of a simple tetrahedron cannot be used directly, since the condition is difficult to check. For voxel and cellular complex representations, the simplest local characterization consists in counting the connected components in the neighborhood of the considered point. In the following, we extend this notion to a TM by using the properties of the homology and relative homology groups of a TM to find a local characterization of simple tetrahedra.

The following theorem is the major result of this paper.

**Theorem 15.** *Let $T$ be a tetrahedron and $O$ a connected set of tetrahedra such that $O \cup T$ is connected. The tetrahedron $T$ is simple if and only if both the attachment set $Bd_s T$ of $T$ and the complement $Bd_b T$ of that set in the boundary of $T$ are non-empty and connected.*

**Proof.** (1) Let us first show that if $O \cup T$ is connected and both the attachment set $Bd_s T$ of $T$ and its complement $Bd_b T$ in $Bd T$ are non-empty and connected, then the inclusion mapping $i: O \to O \cup T$ is a homotopy equivalence.

Since $Bd_b T$ is non-empty, at least one of the four faces of $T$ is not in $Bd_s T$.[3] Let $X$ be the union of the other three faces of $T$. The tetrahedron $T$ can be continuously deformed until it collapses onto $X$.

Now $Bd_s T$ (which is included in $X$) and $X$ are connected subsets of $Bd T$ that have non-empty and connected complements in $Bd T$. It follows that $X$ can be continuously deformed in $Bd_s T$. Thus the tetrahedron $T$ can be continuously deformed in $Bd_s T$. Hence the inclusion mapping is a homotopy equivalence, and $T$ is simple.

(2) Let us now show that if the inclusion mapping $i: O \to O \cup T$ is a homotopy equivalence and $O \cup T$ is connected, then both the attachment set $Bd_s T$ of $T$ and its complement $Bd_b T$ in $Bd T$ are non-empty and connected. This part of the proof is less simple and uses the results of Section 3.

Since the inclusion mapping $i: O \to O \cup T$ is a homotopy equivalence, from Theorem 9, it induces an isomorphism $i_*$ between the homology groups $H_r(O)$ and $H_r(O \cup T)$ for all $r = 0, 1, 2, \ldots$

Since the set $O \cup T$ is connected, we have $H_0(O \cup T) \cong \mathbb{Z}$ (cf. Theorem 8). Also, we know that the homology sequence of $O \cup T$ and $O$ is exact (cf. Theorem 13).

[3] Indeed, if all four faces of $T$ were in $Bd_s T$, then from the definition of shared simplexes, all the subsimplexes of the faces were shared too, and $Bd_b T$ would be empty. If follows that $Bd_b T$ cannot contain only an edge or a vertex.

More precisely, the sequence $\cdots \rightarrow_{i_{r*}} H_r(O \cup T) \rightarrow_{j_{r*}} H_r(O \cup T/O) \rightarrow_{\partial_{r*}} H_{r-1}(O) \rightarrow_{i_{r-1*}} H_{r-1}(O \cup T) \rightarrow_{j_{r-1*}} \cdots \rightarrow_{i_{0*}} H_0(O \cup T)$ is exact.

Since the mappings $i_{r*}: H_r(O) \rightarrow H_r(O \cup T)$ are isomorphisms (cf. Theorem 9), we have $ker\ i_{r*} = \{0\}$. Since $\mathrm{im}\,\partial_{r*} = ker\ i_{r-1*}$(exact homology sequence), we have $H_r(O \cup T/O) = \{0\}$ for all $r$.

Let us now use the notations of Theorem 14 and set $O_K = O \cup T$, $O_L = O$, $O_{K_1} = T$. Since $O \cup T$ is connected, $O_{K_1} = T$ contains $O \cup T - O$. We have $O_{L_1} = Bd_s T$. Thus, applying Theorem 14, we can deduce that the homology groups $H_r(O \cup T/O)$ and $H_r(T/Bd_s T)$ are isomorphic for all $r$. It follows that $H_r(T/Bd_s T) = \{0\}$ for all $r$.

Let us now consider the homology homomorphisms $i_{r*}: H_r(Bd_s T) \rightarrow H_r(T)$ for all $r = 0, 1, 2, \ldots$ induced by the inclusion mapping $i: Bd_s\ T \rightarrow T$. Since $Bd_s T \subseteq T$, the homology sequence $\cdots \rightarrow_{i_{r*}} H_r(T) \rightarrow_{j_{r*}} H_r(T/Bd_s T) \rightarrow_{\partial_{r*}} H_{r-1}(Bd_s T) \rightarrow_{i_{r-1*}} H_{r-1}(T) \rightarrow_{j_{r-1*}} \cdots \rightarrow_{i_{0*}} H_0(T)$ is exact.

Since $H_r(T/Bd_s T) = \{0\}$, $\mathrm{im}\,\partial_{r*} = \{0\}$ and $ker\ j_{r*} = H_r(T)$. Since the sequence is exact, we have $\mathrm{im}\,\partial_{r*} = ker\ i_{r\ -\ 1*} = \{0\}$.

We can deduce from this that the homomorphisms $i_{r*}$ are also isomorphisms for all $r$.

Since:

- $H_r(T) = \{0\}$ for all $r \neq 0$ (cf. Table 1),
- $H_0(T)$ is isomorphic to $\mathbb{Z}$ (cf. Table 1),
- $i_{r*}$ is an isomorphism for all $r$,

$H_r(Bd_s T)$ is isomorphic to $\{0\}$ for all $r \neq 0$ and $H_0(Bd_s T)$ is isomorphic to $\mathbb{Z}$.

In conclusion:

- since $O \cup T$ is connected, $Bd_s T$ is non-empty;
- since $H_0(Bd_s T)$ is isomorphic to $\mathbb{Z}$, $Bd_s T$ is connected (cf. Theorem 8);
- since $H_2(Bd_s T) = Z_2(Bd_s T)$ is isomorphic to $\{0\}$, there is no linear combination of the faces of $Bd_s T$ such that its boundary is null; since $H_2(Bd\,T) = Z_2(Bd\,T)$ is isomorphic to $\mathbb{Z}$ (cf. Table 1), it is possible to build a linear combination of the faces of $Bd\,T$ such that its boundary is null; and since $Bd_s T \subseteq Bd\,T$, there exists at least one face of $Bd\,T$ in $Bd_b T$, so $Bd_b T$ is non-empty;
- since $Bd_s T$ is a polyhedron in $Bd\,T$ (because $Bd_s T$ is connected) and every closed curve of $Bd_s T$ is a border of an element of dimension 2 in $Bd_s T$ (since $H_1(Bd_s T) = \{0\}$), $Bd_b T$ is connected.

Three illustrations of Theorem 15 are given in Fig. 6:

- (a) $Bd_s T = \{(a, b, c) \cup (c, d)\}$; $T$ is simple, because both the attachment set of $T$ and its complement in the boundary of $T$ are non-empty and connected;
- (b) $Bd_s T = \{(a) \cup (c, d)\}$; $T$ is non-simple because its attachment set is not connected;
- (c) $Bd_s T = \{(a, b) \cup (a, c) \cup (b, c, d)\}$; $T$ is non-simple: although its attachment set is connected, its complement in the boundary of $T$ is not connected.

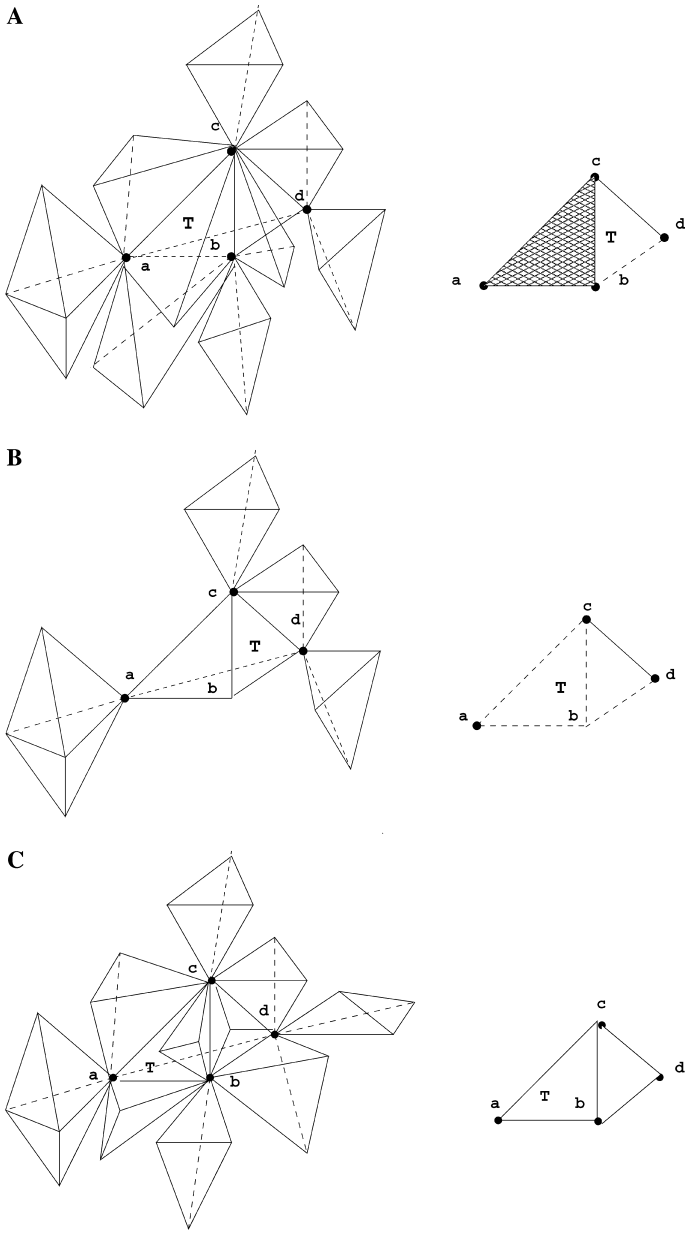


Fig. 6. $T$ is a tetrahedron with vertices $(a, b, c, d)$. The neighborhood $N(T)$ of $T$ is shown on the left and its attachment set $Bd_s T$ is shown on the right.

It should be noted that in the case of voxels, Kong [10] has shown that if $N(T)$ is connected then the attachment set $Bd_s T$ is also connected, which simplifies the characterization. Saha and Majumber [15] have shown that this condition is not

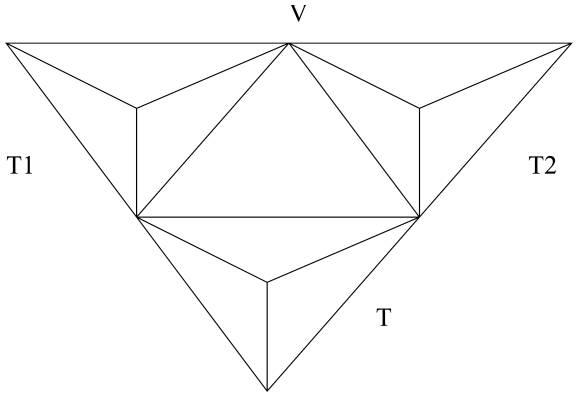


Fig. 7. $N(T) = \{T, T_1, T_2\}$ is connected but $Bd_s T$, which contains only the two shared vertices to $T$ and $T_1$ and $T_2$, respectively, is not connected.

sufficient in the case of tetrahedra. In fact, Fig. 7 is a counter example in which $N(T)$ is connected and $Bd_s T$ is not. □

## 5. Homotopic tetrahedral mesh labeling

As an illustration of our main result, this section addresses the problem of generating 3D finite element (FE) from MRI voxel datasets for applications in brain imaging, such as the one mentioned in introduction, i.e., constructing a realistic model of the head and head tissues for solving the forward and inverse problems in EEG and MEG (see Fig. 3). We describe in this section a meshing method that leads to tetrahedral 3D meshes with well-defined geometric and topological properties. Our algorithm is based on a recursive decomposition of a segmented volume into congruent tetrahedra called almost regular tetrahedrization of $\mathbb{R}^3$ (ART) [16] followed by a mesh labeling procedure under topological constraints. More details can be found in [17]. Although our local characterization could have been incorporated in advancing front approaches (see e.g., [18–21]), it would have been more difficult to guarantee good geometrical properties and would need surface descriptions of the brain structures, which are difficult to obtain with the required topology. Therefore, we rather rely on subdivision approaches.

### 5.1. From a segmented image to an ART

Irregularly shaped tetrahedra cause numerical computation instabilities in finite element methods. Ideally, a FE tetrahedral mesh should consist entirely of equilateral tetrahedra. Unlike in two dimensions, there exists no canonical regular tetrahedrization since one cannot partition $\mathbb{R}^3$ with equilateral tetrahedra. In a previous work [22], we have shown that introducing the notion of invariance under subdivision of a tetrahe-

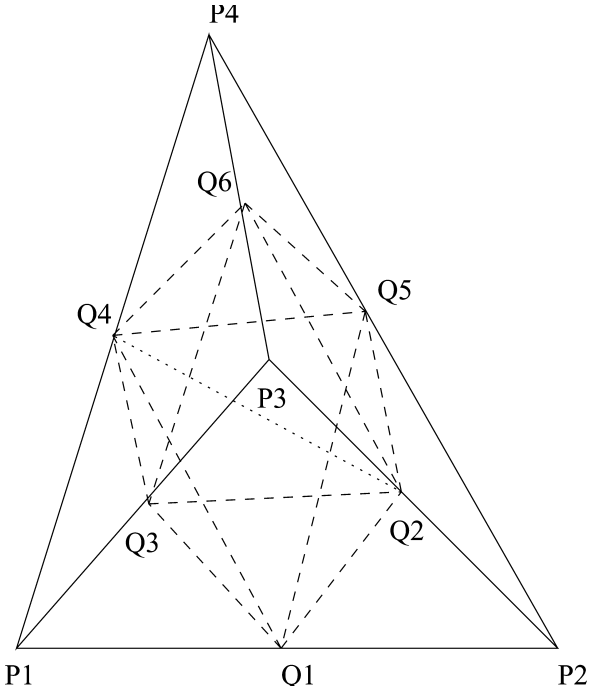


Fig. 8. Subdivision of a tetrahedron $K$.

dron allows to partition $\mathbb{R}^3$ with almost regular tetrahedra. More precisely, if a tetrahedron is split into eight tetrahedra by halving the edges as indicated in Fig. 8, there exists an Euclidean mapping[4] between the vertices of every pair of the small tetrahedra.

We proved that an ART based on tetrahedra which are invariant under subdivision has the following connectivity:

- it has a 4-connectivity for the faces, 18 for the edges and 70 for the vertices;
- each vertex is shared by 24 tetrahedra.

For the sake of stability of any FE computation carried out with tetrahedral elements, the tetrahedra should satisfy some quality criteria. Without error estimator of the problem to be solved, a quality criterion based on the geometric aspect of a tetrahedron is often used. Among all the possible quality measures [23,24], we use the following one:

$$Q_{T_\alpha} = \alpha \frac{h_{\max}}{\rho_T} = \alpha \frac{h_{\max} S_T}{3V_T}, \tag{15}$$

[4] A mapping $M$ so that for all $x$ of $\mathbb{R}^3$ $M(x) = B{\cdot}x + b$ with $B \in \mathbb{R}^3 \times \mathbb{R}^3$ and $b \in \mathbb{R}^3$ is called an Euclidean transformation if and only if $B{\cdot}B^t = Id$ and $M$ is a one-to-one mapping from $\mathbb{R}^3$ to $\mathbb{R}^3$.

where $h_{\max}$ is the largest side of the tetrahedron $T$, $\rho_T$ is the radius of the inscribed sphere of $T$, $S_T$ is the sum of the area $S_i$ of each face of $T$, and $\alpha$ is a normalization coefficient to ensure a quality equal to one for an equilateral tetrahedron ($\alpha = \sqrt{6}/12$).

Thus, as shown in [22], the following tetrahedron $T^*$, invariant under subdivision, has the best quality (the closest to one):

$$T^* = \left\{ \begin{pmatrix} 0 \\ 0 \\ 0 \end{pmatrix}, \begin{pmatrix} 1 \\ 0 \\ 0 \end{pmatrix}, \begin{pmatrix} \frac{1}{3} \\ \frac{2\sqrt{2}}{3} \\ 0 \end{pmatrix}, \begin{pmatrix} \frac{2}{3} \\ \frac{\sqrt{2}}{3} \\ \frac{2}{3} \end{pmatrix} \right\}. \tag{16}$$

From the center of the domain of interest, we define 24 tetrahedra based on $T^*$ sharing this center, which are then recursively subdivided to partition the space at the desired resolution.

An ART mesh based on a segmented image can be split into two distinct parts. The first part describes the geometric structure of the volume mesh and consists of all the ART tetrahedra. Once the geometric construction of an ART is achieved, the labeling of the tetrahedra from a segmented image is only possible if we can compute the proportion of each segmented object in each tetrahedron. By doing so, we can affect the best label object to each tetrahedron (see next subsection). Therefore, the second part consists of the vectors of proportions of each object in each tetrahedron of the ART mesh. Thus, we obtain a discrete image based on tetrahedra.

The segmentation step is outside the scope of this paper, but details can be found in [17,25].

An example of ART construction at different resolutions is shown in Fig. 9.

### 5.2. Homotopic labeling

In this section, we introduce the homotopic labeling algorithm of an ART mesh. This algorithm uses two main functions:

- *initial model:* this function is used to build the initial model which will then be deformed. The topology of the initial model will be preserved during the deformations.
- *selection criterion:* the choice of the tetrahedra which must be modified is done using this function. It allows to guide the deformations towards the desired solution. First, this criterion selects only the simple tetrahedra based on our local characterization (Section 4). This selection guarantees the topology of the model during the labeling procedure. Moreover, the selection criterion is based on two thresholds ($\mu_T$ et $\mu_N$) and a Boolean $\mu_{\max}$. The threshold $\mu_T$ allows for the evolution of the model with respect to the proportion of each object in each tetrahedron. The threshold $\mu_N$ allows for the evolution of the model with respect to the proportion of the tissue in the half, at least, of the neighbors by face of a

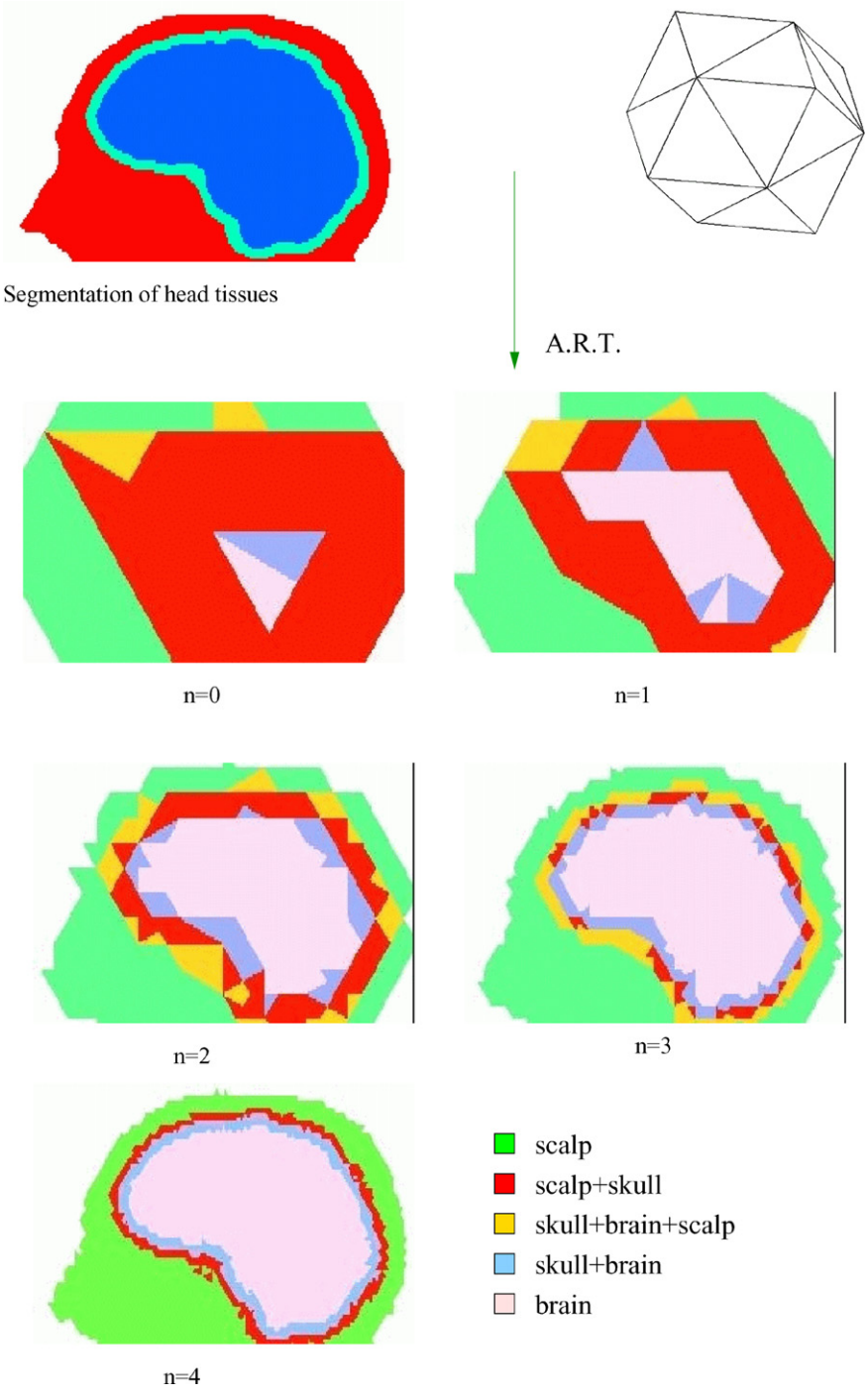


Fig. 9. Successive subdivisions of an ART (only one slice of the 3D volume is shown).

given tetrahedron. Finally, $\mu_{\max}$ allows the evolution of the model with respect to the proportion of each object in the ongoing labeling. This Boolean is true if the object proportion, in the current labeling, is maximum compared to the proportion of the other tissues. Considering neighbors by faces is a restriction (a sub-case) with respect to our characterization, and leaves aside some simple tetrahedra. However, it reduces the number of tetrahedra to be checked, and it leads to more regular meshes, better adapted to the needs of finite element methods.

It is well known that a topology of interwoven spheres [26,27] is a good approximation of the topology of head tissues (brain, skull, and scalp). Therefore, it is necessary to use the homotopic labeling during the meshing process to impose the result of the topology.

The labeling algorithm is applied sequentially on the different objects. First, the algorithm is initialized from a connected object of the interior of the brain. This connected object is simply a tetrahedron labeled as brain. The selection of the tetrahedra, initially in the background, to be modified (i.e., to be added to the brain) is

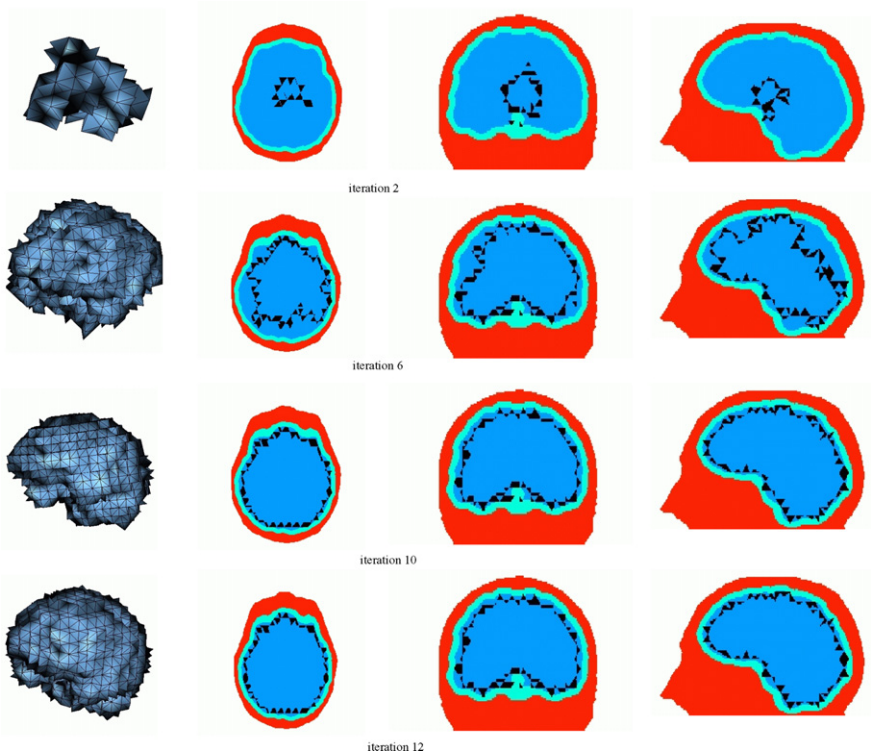


Fig. 10. Homotopic labeling of the brain. Simple tetrahedra are shown in black (superimposed on the head segmentation). A 3D rendering, and axial, frontal, and sagittal slices are shown (from left to right, in each row).

done by analyzing the simple tetrahedra belonging to the brain and the neighbors by face which have a proportion of brain tissue greater than the threshold $\mu_T$. The model does not evolve anymore when the total number of tetrahedra having a proportion of the brain greater than the threshold $\mu_T$ defined in the tetrahedron selection is reached, or when there are no more simple tetrahedra. At the end of this labeling procedure, we obtain a connected object representing the meshed brain. This object does not contain any cavity or tunnel and is homeomorphic to a sphere. This process is illustrated in Fig. 10.

To get the interface for the skull, we consider the union of the skull with the brain as one connected component. Therefore, the connected object obtained for the brain before forms the initial model for the labeling procedure of the skull. The deformation algorithm of the skull detects the simple tetrahedra of the background using the threshold $\mu_T$ which corresponds to the threshold of the proportion of the skull in the simple tetrahedra, the maximal proportion of the skull $\mu_{\max}$ and the threshold $\mu_N$ which corresponds to the proportion of the skull in the neighbors by face of the simple tetrahedra.

Similarly, we consider the union of brain, skull, and scalp as one connected component for the labeling of the scalp and we apply the same labeling algorithm based on our selection criterion.

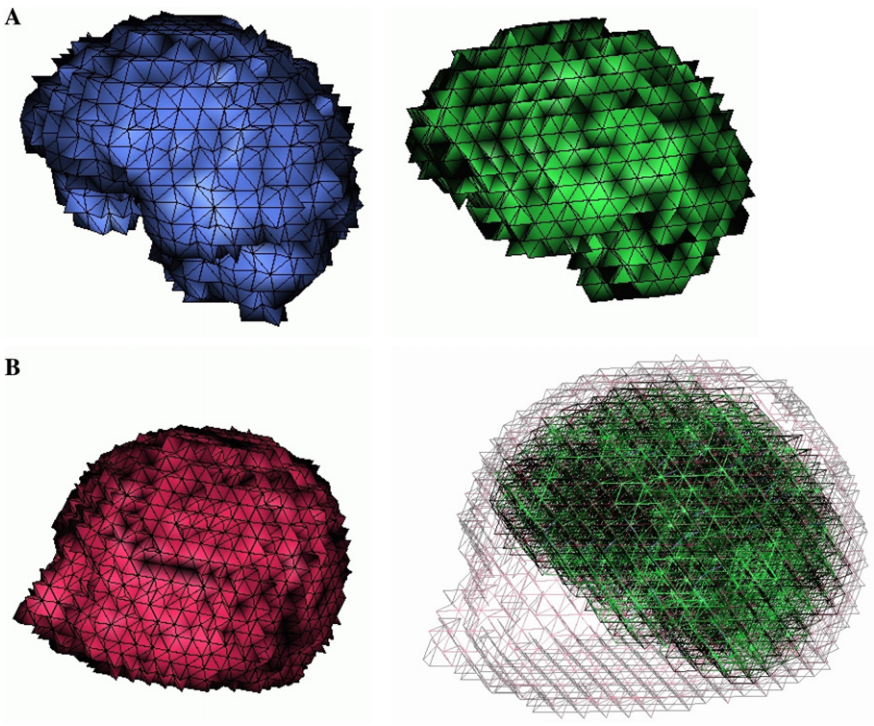


Fig. 11. A 3D representation of an homotopic ART mesh of the head tissues. (A) Skull and brain; (B) scalp and superimposition of all three meshes.

Fig. 11 shows a 3D representation of an homotopic labeling based on an ART mesh of the head tissues.

More details about the choice of the parameters can be found in [17,28,22]. Typical values are $\mu_T = 0.8$ and $\mu_N = 0.6$ to guarantee that the labeled meshed is closed to the segmentation results.

## 6. Conclusion and perspectives

In this paper, we have proved a new characterization of simple elements in a tetrahedral mesh, based on homology theory. Many concepts in this paper depend only on the fact that tetrahedra are convex. Therefore, they can be generalized to representations composed of convex polyhedra.

This characterization applies for one object and the background. Future work aims at extending the characterization to the case of several objects [29,30]. An approach similar to the one developed in [8] for cellular complexes could be investigated too.

From this characterization, we derived a homotopic labeling procedure, and described a method to generate 3D meshes from medical voxels datasets. These meshes are targeted towards applications in the finite element method. Previous approaches [31] required the formation of boundaries and well-defined polyhedral objects which are hard to generate from medical image datasets. Moreover, we can find stability problems of these algorithms applied to highly non-convex objects in the brain. By spatial decomposition into ART of the voxels datasets followed by an homotopic labeling of the ART, we could derive a numerically stable algorithm for the generation of tetrahedral grids. Our primary goal is to construct electromagnetic FE models of the head. These meshes can be used for a number of applications including brain damages mechanical FE models, growth processes in the brain, or irradiation in tumor therapy.

## References

[1] J.K. Udupa, Applications of digital topology in medical three-dimensional imaging, Topol. Appl. 46 (1992) 181–197.
[2] J.D. Boissonnat, Shape reconstruction from planar cross sections, Comput. Vision Graph. Image Process. 44 (1988) 1–29.
[3] G. Marin, Utilisation de la méthode des éléments finis pour le calcul des champs électromagnétiques à l'aide d'un modèle réaliste de tête en MEG et EEG, Ph.D. thesis, Université Paris Sud Orsay, 1997.
[4] G. Bertrand, G. Malandain, A new characterization of three-dimensional simple points, Pattern Recogn. Lett. 15 (1994) 169–175.
[5] T.Y. Kong, A. Rozenfeld, Digital topology: introduction and survey, Comput. Vision Graph. Image Process. 48 (1989) 357–393.
[6] D.G. Morgenthaler, Three dimensional simple points: serial erosion, parallel thinning, and skeletonization, Tech. Rep. TR-1005, Computer Vision Laboratory, Computer Science Center, University of Maryland, College Park, 1981.
[7] Y.F. Tsao, K.S. Fu, A parallel thinning algorithm for 3-D pictures, Comput. Vision Graph. Image Process. 17 (1981) 315–331.

[8] Y. Cointepas, I. Bloch, L. Garnero, Cellular model for multi-objects multi-dimensional homotopic deformations, Pattern Recogn. 34 (9) (2001) 1785–1798.
[9] P.K. Saha, B. Chanda, D.D. Majumder, Principles and algorithms for 2-D and 3-D shrinking, Tech. Rep. TR/KBCS/2/91, Indian Statistical Institute, Calcutta, India, 1991.
[10] T.Y. Kong, On topology preservation in 2D and 3D thinning, Int. J. Pattern Recogn. Artif. Intell. 9 (5) (1995) 813–844.
[11] J.G. Hocking, G.S. Young, Topology, Dover, New York, USA, 1988.
[12] V.A. Kovalevsky, Finite topology as applied to image analysis, Comput. Vision Graph. Image Process. 46 (1989) 141–146.
[13] M. Nakahara, Geometry, Topology and Physics, Adam Hilger, New York, USA, 1990.
[14] T. Ward, Topology lecture notes, Tech. Rep., Computer Vision Laboratory, Computer Science Center, University of East Anglia, School of Mathematics, 2001.
[15] P.K. Saha, D.D. Majumber, Local topological parameters in a tetrahedral representation, Graph. Models Image Process. 60 (1998) 423–436.
[16] A. Fuchs, Optimierung von Delaunay-Triangulierungen, Ph.D. thesis, Fakultät Mathematik Universität Stuttgart, 1996.
[17] J. Pescatore, Maillages homotopiques tétraédriques des tissus de la tête pour le calcul du problème direct en électro/magnéto-encéphalographie, Ph.D. thesis, École Nationale Supérieure des Télécommunications, ENST 2001E034, 2001.
[18] S.H. Lo, A new mesh generation scheme for arbitrary planar domain, Int. J. Numer. Methods Eng. 63 (207) (1985) 141–154.
[19] R. Löhner, Extensions and improvements of the advancing front grid generation technique, Commun. Numer. Methods Eng. 12 (1996) 683–702.
[20] J. Peraire, K. Morgan, Unstructured mesh generation including directional refinement for aerodynamics flow simulation, Finite Elem. Anal. Des. 25 (3–4) (1997) 343–355.
[21] J.R. Sack, J. Urrutia, Handbook of Computational Geometry, North Holland, Amsterdam, 2000.
[22] J. Pescatore, L. Garnero, I. Bloch, Tetrahedral finite element meshes of head tissues from MRI for the MEG/EEG forward problem, in: 12th Scandinavian Conference on Image Analysis, Bergen, Norway, 2001, pp. 71–80.
[23] V.N. Parthasarathy, C.M. Graichen, A.F. Hathaway, A comparison of tetrahedron quality measures, Finite Elem. Anal. Des. 15 (1993) 255–261.
[24] E. Martinez, L. Garnero, I. Bloch, Refined adaptive meshes for the localization of cortical activity, Tech. Rep. 2003D001, Ecole Nationale Supérieure des Télécommunications, 2003.
[25] P. Dokladal, I. Bloch, M. Couprie, D. Ruijters, R. Urtasun, L. Garnero, Topologically controlled segmentation of 3D magnetic resonance images of the head by using morphological operators, Pattern Recogn. 36 (10) (2003) 2463–2478.
[26] J.C.D. Munck, The potential distribution in a layered anisotropic spheroidal volume conductor, J. Appl. Phys. 64 (1988) 464–470.
[27] J. Sarvas, Basic mathematical and electromagnetic concepts of the biomagnetic inverse problem, Phys. Med. Biol. 32 (1) (1987) 11–22.
[28] J. Pescatore, I. Bloch, L. Garnero, Homotopic tetrahedra meshes labeling of head tissues, in: Winterschool Digital and Image Geometry, Daghstul, Germany, 2000, pp. 21–22.
[29] J. Burguet, I. Bloch, Homotopic labeling of elements in a tetrahedral mesh for the head modeling, CIARP, Puebla, Mexico, 2004.
[30] J. Burguet, N. Gadi, I. Bloch, Realistic models of children heads from 3D MRI segmentation and tetrahedral mesh construction, 3DPTV, Thessaloniki, Greece, 2004.
[31] P.J. Frey, P.L. George, Maillages: application aux méthodes d'éléments finis, Hermes, Paris, France, 1999.